Proceedings of the 2023 Design of Medical Devices Conference
DMD2023
April 17-19, 2023, Minneapolis, MN, USA

DMD2023-1689

DESIGN OF FABRIC-REINFORCED POLYURETHANE COMPOSITES FOR AORTIC AND OTHER CARDIAC CONSTRUCTS

Charmaine Nieves
University of Illinois
Champaign, IL

Sandra Edward
University of Illinois
Champaign, IL

Mayura Kulkarni
University of Illinois
Champaign, IL

Holly Golecki
University of Illinois
Champaign, IL

ABSTRACT

When patients experience heart failure, medical devices can support lost cardiac function. However, compliance mismatch between biological tissues and devices present challenges for long term integration. For example, silicone, a common polymer used in soft robotic medical devices, has negative side effects when implanted in vivo. This paper explores biomimetic properties of alternative materials by testing mechanical properties of polyurethane composites. Testing reveals similarities between our composites and native tissues in the heart and aorta. When built into fabric reinforced elastomeric enclosures (fabREEs), our composite actuators behave similar to native aortic tissue. By analyzing hoop and longitudinal stresses in actuators, we present candidate materials for building aortic models for use in transplantations or benchtop testing. We show that these materials can serve to mimic a range of cardiac tissues and that future of medical device design will benefit from considering these soft material composites in new devices.

Keywords: aorta, cardiac structures, elastomer composites, soft robotics

NOMENCLATURE

σ_h	circumferential stress (Pa)
σ_L	longitudinal stress (Pa)
ϵ_h	circumferential strain (m/m)
ϵ_L	longitudinal strain (m/m)
ϵ_C	circumferential area strain (m^2/m^2)
P	pressure (Pa)
r	radius of FabREE (m)
l	length of FabREE (m)
t	thickness of FabREE (m)
E	Young's modulus (Pa)
ν	Poisson's ratio (m/m)

1. INTRODUCTION

Heart disease is the leading cause of death in the United States that may involve complex surgeries to treat patients [1]. Patients with conditions including heart failure may be deemed too high risk for transplants or other surgeries for their conditions. Current commercial mechanical ventricular assist devices extend life for patients but introduce additional risks. For example, patients with heart failure using left-ventricle assistive devices are at risk of thrombosis since this solution interfaces tissues and blood with a mechanical pump [2].

In recent years, the field of soft robotics has introduced a variety of soft material mechanical solutions to address shortcomings of commercially available designs [3]. Direct cardiac compression sleeves are coupled around the exterior of the heart surface, and with pneumatic controls, the devices contract and compress the heart [4]. This device assists enlarged ventricles to pump blood at an improved cardiac output. Materials research has also been conducted using silicone composites to mimic certain structures of the human heart [5]. Soft material ventricular assist devices may improve the bridge-to-transplant options for some patients.

When patients can receive a transplant, the donated organ is transplanted to the patient via SherpaPak™ Cardiac Transport Systemor similar device. During organ transportation, a beating perfused state is used to improve outcomes after transplantation and blood outlet tubing is secured to the organ during transportation [6]. This tubing replaces the function of the aorta in vivo. The aorta is composed of compliant tissue that expands to fill with blood during systole, so that during diastole, it can relax and provide constant blood pressure throughout the body. During transplant, a compliant and ductile material is needed for interfacing the device with soft tissues to prevent injury to the tissue. If the properties match aortic tissue, it can also serve the fluid dynamics functions of the aorta according to the Windkessel Effect [7]. In one study, silicone composites were

able to mimic the mechanical behavior of aortic tissue [5]. However, silicone materials have been demonstrated to have side effects when implanted inside the human body [8]. Medical mesh-silicone composites have also been tested for mechanical failure and biocompatibility with cardiac tissues surrounding the heart [9]. With previous research, it has been determined silicone composites are able to mimic cardiac structures' properties but introduce implantation risks.

Polyurethane elastomers have not been fully explored in this research area, even though polyurethane is used for current medical devices including the pacemaker leads due to the material's biocompatibility and mechanical properties [10]. Polyurethane has material behavior like silicone and may serve as an alternative material for future mechanical soft material solutions in cardiac applications. The history and challenges in this field of cardiac assist device development lead us to ask: How do the mechanical properties of polyurethane composites compare to silicone composites and cardiac tissues and is it possible to create a model aorta from these materials?

2. MATERIALS AND METHODS

To determine if polyurethane composites may be used to safely interface with cardiac tissue, we built a variety of composite materials, tested their mechanical properties, and compared them to biological tissues. After selecting candidates for cardiac interfacing devices, we built an aortic model using actuator fabrication methods to evaluate properties of the elastomer composite cylindrical constructs.

2.1 Composite Molding

Polyurethane rubber (Smooth-On) was mixed in 1:1 ratio as indicated by the manufacturer and degassed to prevent air voids in the sample that may lead to lower tensile strength or failure. Composites were fabricated in a multistep process. First, an elastomer layer (1mm) was cast and air cured. Next, liquid elastomer was brushed on fabrics and placed on top of the first elastomer layer. After curing, a second elastomer layer was cast on top of the fabric and air cured. For mechanical testing, composites were molded in a dog bone shape (Figure 1).

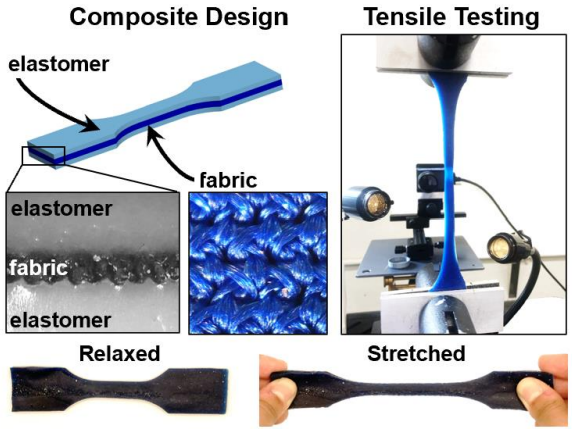

FIGURE 1: COMPOSITE DESIGN AND TENSILE TESTING SETUP FOR FABRIC-REINFORCED URETHANE ELASTOMERS

The elastomer materials used to create composites included Vytaflex 10 and Reoflex 20 polyurethanes and EcoFlex 00-30 silicone. Fabric composites were built with textiles composed of (1) 80% nylon/20% spandex ("80% Nylon"), (2) 89% nylon/11% spandex ("89% Nylon"), and (3) 95% rayon/5% spandex ("Rayon"). Each elastomer and composite combination were molded separately resulting in a total of 12 samples.

2.2 Composite Mechanical Testing

Samples were tested using an MTS Criterion Model 43 tensile testing machine at a strain rate of 10mm/min [5]. Samples had a gage length of approximately 25 mm, thickness of 2.5 mm, width of 25 mm in the gage region, and total length of 130 mm. All samples were tested to 80 mm. Force-displacement data was used to generate stress-strain curves shown in Figure 2.

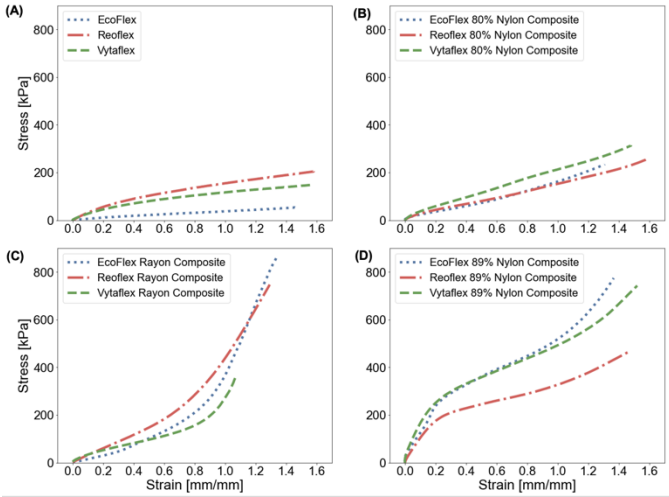

FIGURE 2: STRESS-STRAIN CURVES FOR (A) ELASTOMERS, (B) 80% NYLON COMPOSITES, (C) RAYON COMPOSITES AND (D) 89% NYLON COMPOSITES

Simultaneously, digital image correlation software (VIC 2D Correlated Solutions) was used to track displacement of small, sprayed marks in the longitudinal and axial direction. These displacements were used to calculate Poisson's ratio (Table 1).

TABLE 1: POISSON RATIO AND YOUNGS MODULUS OF COMPOSITE MATERIALS

Sample	Poisson Ratio, ν	Youngs Modulus, E[kPa]
EcoFlex 0030	0.40	53.99
EcoFlex 0030 80% Nylon	0.24	178.74
EcoFlex 0030 Rayon	…	…
EcoFlex 0030 89% Nylon	0.33	1044.97
Reoflex 20	0.39	263.29
Reoflex 20 80% Nylon	0.25	210.26
Reoflex 20 Rayon	0.38	302.24
Reoflex 20 89% Nylon	0.11	1132.64
Vytaflex 10	0.44	216.19
Vytaflex 10 80% Nylon	0.37	286.85
Vytaflex 10 Rayon	0.43	254.87
Vytaflex 10 89% Nylon	0.06	1189.53

2.3 Fabrication of FabREEs

We then fabricated fabric-reinforced elastomeric enclosures (fabREEs) to model an aorta for incorporation into cardiac support technologies including tubing that connects donor hearts to perfusion systems. fabREEs are tubular structures composed of elastomers that expand and bend based on engineered fiber weaves, in our case manufactured woven textiles. fabREEs are cylindrical in shape when deflated. When pressurized air is passed through the inlet of the fabREE, it inflates, increasing diameter and length as depicted in Figure 3.

FabREEs were fabricated using 3D printed cylindrical molds. Polyurethane and silicone elastomers were each mixed according to manufacturer protocols and cast in molds. A 9 mm steel rod was inserted through its center to create the hollow internal cavity of the FabREE where pressurized air passes through. The structures were then air-cured. The composite structures for each material were created by brushing liquid elastomer onto the fabric, wrapping the fabric around the FabREE, and air-curing.

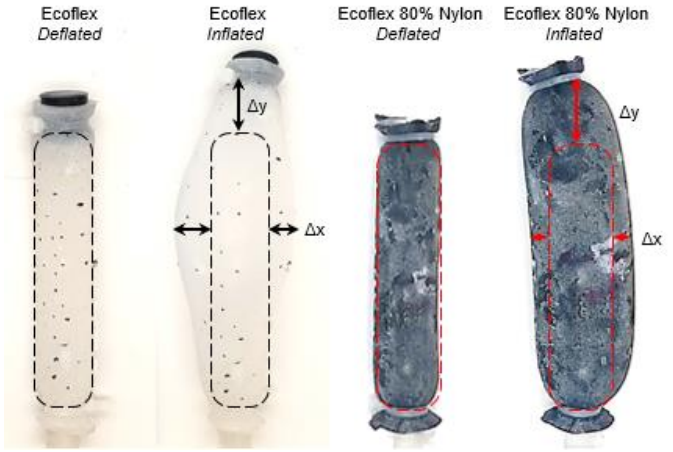

FIGURE 3: IMAGES OF FABREES IN EXPANDED AND RELAXED STATES: ECOFLEX 80% NYLON UNINFLATED (LEFT) AND INFLATED (RIGHT).

2.4 Testing of FabREEs

As mentioned earlier, the function of the aorta is to expand radially and hold a volume of blood until diastole. To understand the properties of these materials for use as aortic mimics, the circumferential and longitudinal stress and strain values for each fabREE composite were theoretically and experimentally determined. As fabricated, the construct original radius, longitudinal length, and thickness were measured. We observed that elastomers and composite structures had some variability in thicknesses upon curing and demolding attributed to fabric variations. fabREEs were inflated to 15 kPa pressure to match the pressure experienced in the aorta in vivo (P=10.6-16 kPa) [11]. As inflated, radius and longitudinal lengths were measured.

Theoretical values of hoop stress (Equation 1), longitudinal stress (Equation 2), circumferential strain (Equation 3), and longitudinal strain (Equation 4) are defined by the following equations:

$$\sigma_H = \frac{Pr}{t} \tag{1}$$

$$\sigma_L = \frac{Pr}{2t} \tag{2}$$

$$\epsilon_C = \frac{Pr}{Et}\left(1 - \frac{\nu}{2}\right) \tag{3}$$

$$\epsilon_L = \frac{Pr}{Et}\left(\frac{1}{2} - \nu\right) \tag{4}$$

Theoretical hoop stress and longitudinal stress values for all material FabREEs varied based upon construct thicknesses. The hoop strain and the longitudinal strain values were experimentally measured by inflating each of the structures using a pump. Experimental hoop and longitudinal strain values were measured and compared to theoretical values. Circumferential area strain was also measured by the change in area of the fabREE according to Equation 5:

$$\epsilon_{CA} = \frac{A_{inflated} - A_{uninflated}}{A_{uninflated}} = \frac{r^2 - r_0^2}{r_0^2} \tag{5}$$

Theoretical hoop strain and longitudinal strain values were compared with the experimental values. Hoop strain and longitudinal strain values were also compared with the stress and strain of the aorta to determine which materials most closely replicated aortic behavior.

3. RESULTS AND DISCUSSION

3.1 Composite Stiffness

Stiffness data for tested samples shows that composite behavior is influenced by elastomer-fabric adhesion as well as fabric and fiber properties. Young's modulus of polyurethane samples ranged from approximately E=60-2000 kPa as shown in Figure 4. Nylon 89% fabric composites have the highest stiffness of materials tested. While Vytaflex was the second stiffest pure elastomer, it was the stiffest fabric-reinforced composite when 89% nylon fabric was used. This may be explained by adhesion between Vytaflex and the 89% nylon compared to Reoflex or EcoFlex. Rayon materials exhibited bi-modal behavior when past 100% strain, the stiffness Rayon exhibited increasing stiffness, behavior not observed in Nylon samples. Rayon is composed of natural fibers that commonly exhibit bimodal behavior. When selecting a composite for organ or tissue models and devices, the properties of synthetic materials can be tuned based on the healthy or diseased state being modeled.

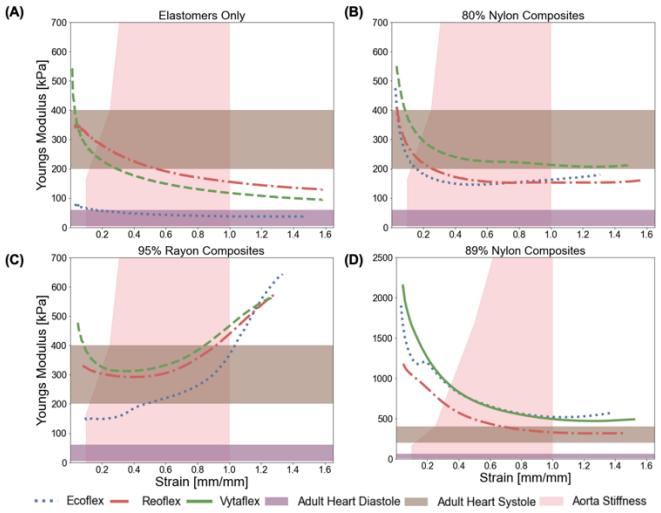

FIGURE 4: YOUNG'S MODULUS OF POLYURETHANE CARDIAC STRUCTURES AND (A) ELASTOMERS, (B) 80% NYLON COMPOSITES, (C) 95% RAYON COMPOSITES AND (D) 89% NYLON COMPOSITES

During tensile testing, Vytaflex-Rayon fabric reinforcement tore near the center of the gage region (Shown in Figure 1). When the fabric itself was tested, the fabric did not fail under similar forces. It was observed that the material edges curled toward the center and created a cupping shape. This bending helped relieve the stress in the fabric and prevent failure during tensile testing when fabrics were tested individually (data not shown). When composite samples were stretched during tensile testing, stress concentrations occurred at the edges. In the case of Vytaflex-Rayon, fabric movement was constrained, and cupping was prevented in the composite. During qualitative exploration, the fabric was easy to tear at the edges. The constrained edges for the Vytaflex led to higher stress concentrations that facilitated tears from the edge to the center of the gage region.

When comparing our composites to biological tissues, most of the urethane samples were within the range of the adult heart's stiffness during systole (E~200-500kPa) [12] at strain values lower than ε=40%. At higher strains, the Young's Modulus decreased for the 80% nylon composites, and they fell in the transition region between the stiffness of the adult heart in diastole and the lower limit of reported aorta stiffness. EcoFlex and the EcoFlex-80% Nylon composite matched adult heart diastole stiffness region (E~5-60kPa) [12] for the strain region tested. Rayon composites matched the heart systole region and began transitioning to aorta stiffness region. These samples mimicked the increased stiffness with higher strains characteristic of aortic tissue reported in literature.

Considering stiffnesses as a design choice for cardiac applications, Reoflex-Rayon composite is broadly suitable for most cardiac applications we considered. Reoflex-Rayon was within the range of both the stiffest stage of heart contraction and extraction. It also fell within the aortic stiffness region that increases at higher strain values, as observed inside the human body, E= 165 kPa - 3.708 MPa at strains from 10% to 100% [5]. Urethane rayon samples replicated the stiffness range of biological cardiac tissues, but at higher strains were not able to increase as expected based on previous in vivo studies of the aorta. The tensile testing provides insight into the Young's Modulus and Poisson ratio behavior of the urethane samples, but for the studying behavior of the samples in implanted situations requiring cylindrical structures such as aortas, a hoop stress study provides more insight regarding stress and strains for these structures.

3.2 Strains in 3D Elastomeric Enclosures

Raw data from the testing methodology described in Section 2.4 was used to calculate the hoop stress and longitudinal stress in FabREE constructs with internal pressures of P=15 kPa using Equation 1 and 2. Figure 5 displays the values of hoop stress and longitudinal stress for each material combination. Although none of the FabREEs reach the same level of circumferential stress experienced by the aorta (σ=45-150 kPa) [13] under the same conditions, most of the materials come close. Most of FabREEs instead experience a similar circumferential stress to the carotid artery (~30-75 kPa) [13]. However, since the calculated stresses depend on variables such as physical dimensions of radius and thickness of the fabREE, most of this can be controlled with dimensioning to achieve desired mechanics.

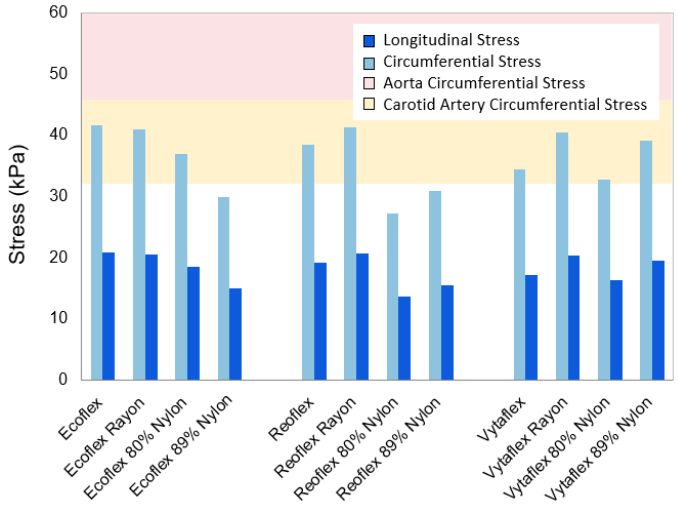

FIGURE 5: HOOP STRESS AND LONGITUDINAL STRESS FOR FABREES WITH PUBLISHED AORTA RANGE AND CAROTID ARTERY RANGE DATA

Next, theoretical circumferential and longitudinal strains in FabREEs were calculated using Equations 3 and 4. Theoretical values were compared to corresponding experimental values. The theoretical circumferential area strains were also calculated using Equation 5.

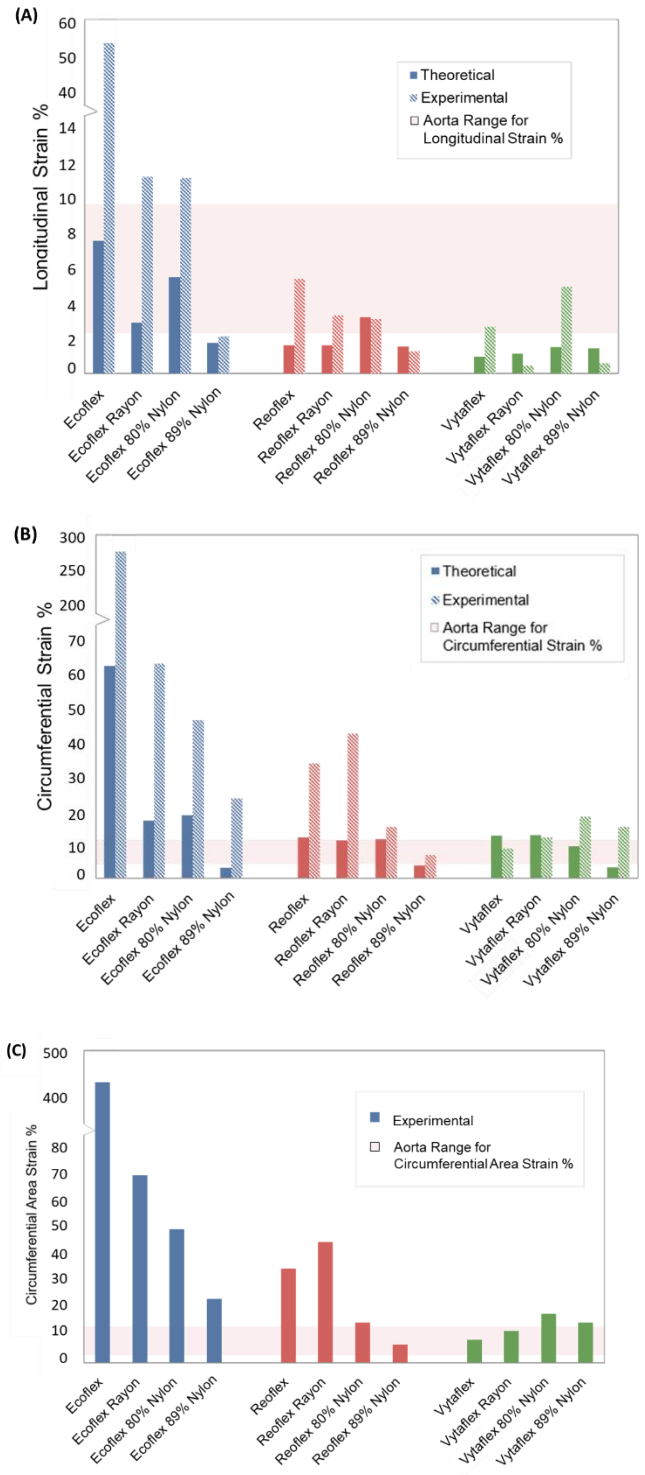

FIGURE 6: (A) HOOP STRAIN, (B) LONGITUDINAL STRAIN, AND (C) CIRCUMFERENTIAL AREA STRAIN PLOTTED WITH THE CORRESPONDING AORTA DATA RANGE

In Figure 6, polyurethane samples and composites had lower longitudinal strain, circumferential strain and circumferential area strain values compared to silicone EcoFlex and EcoFlex composite fabREEs. The longitudinal strain of the ascending aorta ranges from ε~ 5-10.3% [14]. Comparing aortic data with experimental and theoretical values for all fabREEs, we find that the experimental longitudinal strain data for Reoflex and Vytaflex 80% nylon composites most closely fall within the aortic range.

Circumferential strain of the ascending aorta ranges from ε~ 4-10% [15]. Most of the theoretical circumferential strain data for Reoflex and Vytaflex fall within or close to that range. Any of the Vytaflex composite fabREEs are viable options that match the aortic range. Reoflex composites with 80% or 89% Nylon also fall within the range. Similar results are seen in the circumferential area strain data where the aortic ranges lie between ε~5.7-10.4% [14]. Vytaflex composite fabREEs and Reoflex composite fabREEs with 80% or 89% nylon fall within the aortic range. Looking at overall aorta range matching for longitudinal strains, circumferential strains, and circumferential area strains, the Vytaflex 80% nylon composite fabREE matches the aorta data most closely across all working conditions.

As shown in Figure 6, the experimental longitudinal strain and circumferential strain values for all materials were significantly higher than their theoretical values due to the elastomeric properties of the materials. To understand why some differences between theoretical and experimental strain values were higher for some composite fabREEs compared to others, we plotted a general trend of the difference between experimental and theoretical strain values versus the stiffness of the material accounted by its Young's modulus (Figure 7). We normalized all fabREE experimental and theoretical differences with the smallest difference value of 1. The smallest difference strain values for the longitudinal strain was Reoflex 80% Nylon and Vytaflex Rayon for circumferential strains. The normalized difference between experimental and theoretical values for circumferential strain and longitudinal strain values seem to reduce as the stiffness of the material increases, as depicted by the power trendlines in Figure 7. Each of the points for all fabREEs where then grouped by their base elastomer material. We also observe that all 89% Nylon composites group better with each other instead of with their corresponding materials as their stiffness is much higher due to the 89% nylon material.

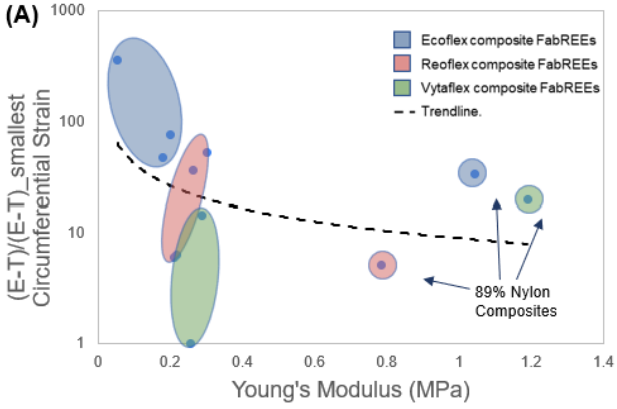

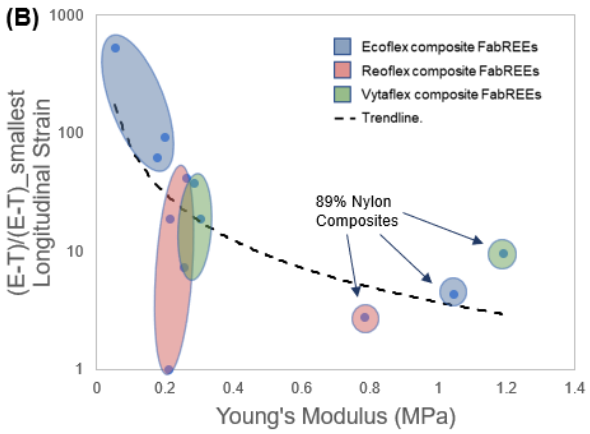

FIGURE 7: DEPICTION OF THE TREND OF DECREASING NORMALIZED DIFFERENCE BETWEEN EXPERIMENTAL AND THEORETICAL VALUES OF (A) CIRCUMFERENTIAL STRAIN AND (B) LONGITUDINAL STRAIN WITH INCREASING MATERIAL STIFFNESS (EXCLUDING 89% NYLON COMPOSITES).

4. CONCLUSION

The results from this study demonstrated the possibility of substituting urethane as an elastomer base for soft robotics cardiac applications to mimic cardiac structures. This opens the possibility to build benchtop aortic models for future testing of organ transplant structures, with Vytaflex 80% nylon composite fabREEs matching aortic behaviors most closely. It also paves the way for future development of cardiac sleeve structures with a fabric-reinforced polyurethane as the base for the sleeve or the actuators for direct cardiac compression for heart failure patients.

ACKNOWLEDGEMENTS

The authors acknowledge Professor Girish Krishnan for sharing elastomer enclosure molds and designs for this work. The authors thank Trisha Patnaik for assistance with data collection. Tensile testing and digital image correlation for urethane samples was carried out in part in the Advanced Materials Testing and Evaluation Laboratory, Materials Research Laboratory, University of Illinois. The project was funded in part by the Henry Lu Foundation and the National Science Foundation EFRI REM grant #1830896.

REFERENCES

[1] Centers for Disease Control and Prevention, "Heart disease Facts," *Centers for Disease Control and Prevention*, Sep. 27, 2021. https://www.cdc.gov/heartdisease/facts.htm

[2] J. Fatullayev, M. Samak, A. Sabashnikov, M. Zeriouh, P. B. Rahmanian, Y.-H. Choi, B. Schmack, K. Kallenbach, A. Ruhparwar, K. Eghbalzadeh, P. M. Dohmen, M. Karck, J. Wippermann, T. Wahlers, A.-F. Popov, A. R. Simon, and A. Weymann, "Continuous-flow left ventricular assist device thrombosis: A danger foreseen is a danger avoided," *Medical Science Monitor Basic Research*, vol. 21, pp. 141–144, 2015.

[3] J. Bonnemain, P. J. del Nido, and E. T. Roche, "Direct cardiac compression devices to augment heart biomechanics and function," *Annual Review of Biomedical Engineering*, vol. 24, no. 1, pp. 137–156, 2022.

[4] M. A. Horvath, E. T. Roche, D. M. Vogt, D. J. Mooney, F. A. Pigula, and C. J. Walsh, "Soft pressure sensing sleeve for direct cardiac compression device," Volume 3: 17th International Conference on Advanced Vehicle Technologies; 12th International Conference on Design Education; 8th Frontiers in Biomedical Devices, 2015.

[5] D. Zhalmuratova, T.-G. La, K. T.-T. Yu, A. R. Szojka, S. H. Andrews, A. B. Adesida, C.-il Kim, D. S. Nobes, D. H. FabREEd, and H.-J. Chung, "Mimicking 'J-shaped' and anisotropic stress–strain behavior of human and porcine aorta by fabric-reinforced elastomer composites," *ACS Applied Materials Interfaces*, vol. 11, no. 36, pp. 33323–33335, 2019.

[6] D. E. Smith, Z. N. Kon, J. A. Carillo, S. Chen, C. G. Gidea, G. L. Piper, A. Reyentovich, R. A. Montgomery, A. C. Galloway, and N. Moazami, "Early experience with donation after circulatory death heart transplantation using normothermic regional perfusion in the United States," *The Journal of Thoracic and Cardiovascular Surgery*, vol. 164, no. 2, 2022.

[7] C. C. Mei, J. Zhang, and H. X. Jing, "Fluid Mechanics of Windkessel effect," *Medical & Biological Engineering; Computing*, vol. 56, no. 8, pp. 1357–1366, 2018.

[8] M. Lee, G. Ponraja, K. McLeod, and S. Chong, "Breast Implant Illness: A Biofilm Hypothesis," *Plastic and Reconstructive Surgery Global Open*, vol. 8, no. 4, Apr. 2020, doi: https://doi.org/10.1097/GOX.0000000000002755.

[9] M. A. Horvath, C. E. Varela, E. B. Dolan, W. Whyte, D. S. Monahan, C. J. Payne, I. A. Wamala, N. V. Vasilyev, F. A. Pigula, D. J. Mooney, C. J. Walsh, G. P. Duffy, and E. T. Roche, "Towards alternative approaches for coupling of a soft robotic sleeve to the heart," *Annals of Biomedical Engineering*, vol. 46, no. 10, pp. 1534–1547, 2018.

[10] S. Wendels and L. Avérous, "Biobased Polyurethanes for Biomedical Applications," *Bioactive Materials*, vol. 6, no. 4, pp. 1083–1106, 2021.

[11] B. D. Hoit, "Normal cardiac physiology and ventricular function," *Reference Module in Biomedical Sciences*, 2014.

[12] R. Emig, C. M. Zgierski-Johnston, V. Timmermann, A. J. Taberner, M. P. Nash, P. Kohl, and R. Peyronnet, "Passive myocardial mechanical properties: Meaning, measurement, models," *Biophysical Reviews*, vol. 13, no. 5, pp. 587–610, 2021.

[13] H. Åstrand, Å. Rydén-Ahlgren, G. Sundkvist, T. Sandgren, and T. Länne, "Reduced aortic wall stress in diabetes mellitus," *European Journal of Vascular and Endovascular Surgery*, vol. 33, no. 5, pp. 592–598, 2007.

[14] V. Bell, W. A. Mitchell, S. Sigurðsson, J. J. Westenberg, J. D. Gotal, A. A. Torjesen, T. Aspelund, L. J. Launer, A. de Roos, V. Gudnason, T. B. Harris, and G. F. Mitchell, "Longitudinal and circumferential strain of the proximal aorta," *Journal of the American Heart Association*, vol. 3, no. 6, 2014.

[15] H. de Hoop, N. J. Petterson, F. N. van de Vosse, M. R. van Sambeek, H.-M. Schwab, and R. G. Lopata, "Multiperspective ultrasound strain imaging of the abdominal aorta," *IEEE Transactions on Medical Imaging*, vol. 39, no. 11, pp. 3714–3724, 2020.